



Air quality improvement assessment and exposure risk of Shandong Province in China during 2014 to 2020

N. N. Wang¹ · C. Y. Zhu¹ · Wei Li¹ · M. Y. Qiu² · B. L. Wang¹ · X. Y. Li¹ · B. D. Jiang¹ · X. Y. Qu¹ · Z. S. Li¹ · H. C. Cheng³

Received: 24 December 2021 / Revised: 11 May 2022 / Accepted: 7 November 2022 / Published online: 19 December 2022

© The Author(s) under exclusive licence to Iranian Society of Environmentalists (IRSEN) and Science and Research Branch, Islamic Azad University 2022

Abstract

As one of the most polluted provinces in China, air pollution events occur frequently in Shandong. Based on the hourly (or daily) concentrations of six air pollutants (PM_{2.5}, PM₁₀, O₃, NO₂, SO₂ and CO), the situations of air quality improvement in three kinds of cities (key cities, coastal cities and general cities) are assessed comprehensively during 2014–2020. Contrary to the daily maximum 8-h average ozone (MDA8 O₃), the annual average concentrations of other pollutants show the downward trends during 2014–2020. Therein, the improvement rates of annual average concentrations of air pollutants in key cities are highest. By 2020, the day proportions of O₃ as the primary pollutant are up to 38% in three kinds of cities. Besides, due to the impact of COVID-19, the monthly average concentrations of PM_{2.5}, PM₁₀, NO₂, SO₂ and CO in February 2020 decrease by 32.1–49.5% year-on-year. There are still about 50% of population exposed to high-risk regions ($R_i > 2$), which are mainly concentrated in main urban areas and industrial areas. Thus, the adjustment of industrial structure and energy composition in the context of carbon peak and carbon neutrality should be implemented in the future.

Keywords Air quality composite index (AQCI) · Primary pollutant · Population exposure risk · Shandong

Introduction

Long-term exposure to ambient air pollution has significantly adverse effects on physical and mental health (Stafoggia et al. 2014). There are about 1.8 million premature mortalities estimated to be attributable to PM_{2.5} exposures in 2017 (Liu et al. 2021). Therein, Shandong is regarded as the second province with the highest premature mortality (about 140 thousand deaths per year) in China (Liu et al., 2016, 2021).

Presently, the researches on the regional distribution characteristics of air pollution are mainly concentrated in Beijing–Tianjin–Hebei region (Xiao et al. 2020; Zhang and Pan 2020a), the Yangtze River Delta region (Ma et al. 2019), Northeast China (Gao et al. 2020), Fen-Wei Plains (Wang et al. 2020), Cheng-Yu Region (Liao et al. 2018), etc. Due to the differences in diffusion conditions influenced by the meteorological and geographical factors and emission levels affected by industrial structures, economic levels, etc., the air pollution in various regions of China also presents different temporal and spatial distribution characteristics (Liu et al. 2020). Generally, the concentrations of PM_{2.5}, PM₁₀, NO₂, SO₂ and CO are the highest in winter and the lowest in summer, while the O₃ concentration peaks in spring and summer (Li et al. 2019b). Besides, the boundary of population density named by Hu Huanyong Line is of great significance in the research on spatial distribution of air pollution. Specifically, more serious air pollution is founded in East of the Hu Huanyong Line, compared with those in West of the Hu Huanyong Line (Huang et al. 2018). With the implementation of the policies and programs about environmental protection and governance, a great progress has been made in particulate matter (PM) governance in certain regions of China (e.g., Beijing–Tianjin–Hebei region, Yangtze River

Editorial responsibility: Samareh Mirkia.

✉ C. Y. Zhu
zchy@qlu.edu.cn

¹ College of Environmental Science and Engineering, Qilu University of Technology (Shandong Academy of Sciences), Jinan 250353, People's Republic of China

² State Grid of China Technology College, State Grid, Jinan 250002, People's Republic of China

³ Weifang Municipal Ecology and Environment Bureau Shouguang Branch, Weifang 262700, People's Republic of China



Delta). For example, the average annual concentrations of $PM_{2.5}$ in Beijing decrease from 85.9 in 2014 to 38.0 $\mu\text{g}/\text{m}^3$ in 2020, with an annual decline rate approximately 12.7% (MEEB 2020). However, O_3 has displaced $PM_{2.5}$ as the primary air pollutant since 2016 in the economically developed areas of China (e.g., Pearl River Delta) (Zhang et al. 2021).

As one of the most polluted areas in China, the proportion of days with grade I and II air quality in Shandong Province is less than 60%, which is far below the national average value (78.8%) in 2016 (MEEC 2016). Therein, five cities, including Binzhou, Liaocheng, Zaozhuang, Jinan and Zibo, are listed in the top 20 cities with the worst air quality issued by Ministry of Ecology and Environmental of the People's Republic of China (MEEC) in 2020 (MEEC 2020). Nevertheless, little research has been done about the spatial and temporal distribution characteristics of mass concentrations of air pollutants in Shandong. Furthermore, the study on urban Comprehensive Air Pollution Index (AQCI) variation and population exposure risk to $PM_{2.5}$ are limited.

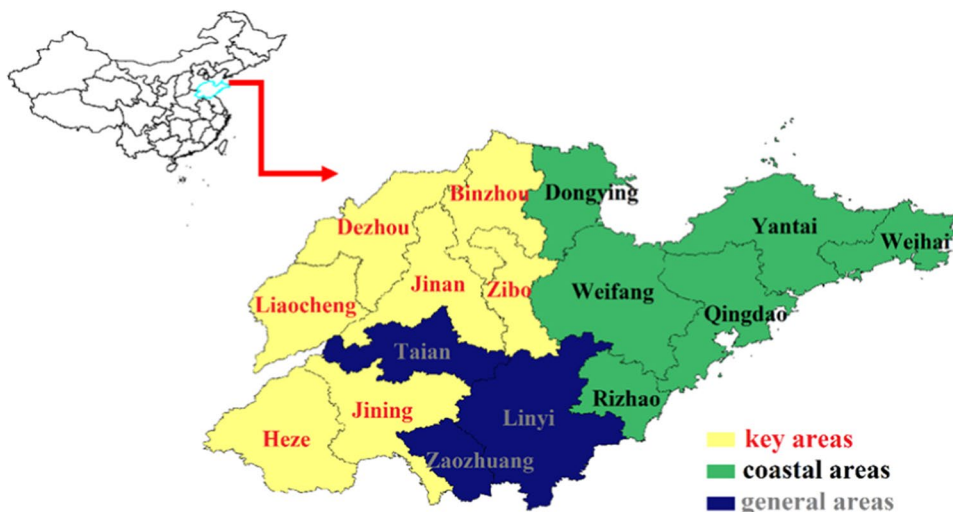
In this study, the hourly (or daily) concentrations of six air pollutants ($PM_{2.5}$, PM_{10} , O_3 , NO_2 , SO_2 and CO) in state controlling air sampling sites of 16 cities in Shandong province during 2014 to 2020 are analyzed statistically in terms of the pollution situation and the spatiotemporal distribution characteristics. In order to further display the pollution characteristics in different kinds of cities, the proportions of different primary pollutants and monthly urban AQCI values in key cities, coastal cities and general cities are discussed in details. Finally, the adverse impacts on exposed people in $PM_{2.5}$ pollution are assessed by using of grid population data and grid $PM_{2.5}$ concentration data. It is hoped that the study can provide the data support for the relevant departments to carry out the air pollution control and prevent.

Materials and methods

Study area

As one of most polluted provinces in China, Shandong is located on the North China plain and nearby Beijing–Tianjin–Hebei region (see Fig. 1), which is regarded as one of provinces with highest population amount and largest coal combustion, as well as most complete industrial categories (Zhou et al. 2015). For instance, GDP and population amount of Shandong in 2020 are estimated at about RMB 7.3 trillion and 101.7 million, accounting for approximately 7.2% and 7.2% of national total, respectively (NSBC 2021). Linyi (11.0 million), Qingdao (10.1 million) and Jinan (9.2 million) are the top three populous cities in Shandong, accounting for about 10.8%, 9.9% and 9.1% of provincial total in 2020, respectively (SPBS 2021). The administrative division of Shandong is adjusted in 2019, and now sixteen cities are under Shandong jurisdiction, including Binzhou, Dezhou, Jinan, Jining, Heze, Liaocheng, Zibo, Dongying, Qingdao, Rizhao, Weifang, Weihai, Yantai, Linyi, Taian and Zaozhuang. Therein, Binzhou, Dezhou, Jinan, Jining, Heze, Liaocheng and Zibo are listed in “2 + 26” cities, which are defined as the air pollution transmission channel cities of Beijing–Tianjin–Hebei region (one of the most seriously contaminated areas of PM pollution). Combined with the geographical characteristics and actual situation of air pollution control in Shandong, there are three categories of cities are involved in this study, including key cities (Binzhou, Dezhou, Jinan, Jining, Heze, Liaocheng and Zibo), coastal cities (Dongying, Qingdao, Rizhao, Weifang, Weihai and Yantai) and general cities (Linyi, Taian and Zaozhuang).

Fig. 1 Geographical distribution of study area and city classifications



Methods

Air quality composite index (AQCI)

Air quality composite index (AQCI) is a dimensionless value describing the comprehensive status of the city's ambient air quality, determined by summing the individual indices of six air pollutants (PM₁₀, PM_{2.5}, SO₂, NO₂, CO and O₃), the bigger AQCI value, the greater comprehensive pollution level (Ye et al. 2018). The individual index I_i of pollutant i is calculated according to Eq. 1:

$$I_i = \frac{C_i}{S_i} \quad (1)$$

where C_i represents the pollutant i concentration, if i is SO₂, NO₂, PM₁₀ or PM_{2.5}, C_i is the monthly average concentration; if i is CO, C_i is the 95th percentile of the daily mean concentration; if i is O₃, C_i is the 90th percentile of the daily maximum 8-h average (MDA8) O₃ concentration. S_i represents secondary standard limit (for SO₂, NO₂, PM₁₀ and PM_{2.5}: annual mean concentration limit; for CO: daily average concentration limit; for O₃: MDA8 O₃ concentration limit). I_{sum} for pollutant i (AQCI) is calculated according to Eq. 2:

$$I_{sum} = \sum_{i=1}^6 I_i \quad (2)$$

Population exposure risk (R_i)

Air quality has an important impact on human health. We propose the indicator of population exposure risk (R_i) to characterize the amount and level of population that are affected by PM_{2.5} air pollution for 16 cities in Shandong (Zhang and Pan 2020b). R_i is defined as follows:

$$R_i = \frac{POP_i \times C_i}{\sum_{i=1}^n POP_i \times \frac{C_i}{n}} \quad (3)$$

where R_i represents the PM_{2.5} population exposure risk in grid i ; POP_i is the population in grid i ; C_i is the PM_{2.5} mass concentration value in grid i ; n is the sum of grids in the study area.

Data sources

In this study, the hourly monitoring data of six regulated air pollutants (PM_{2.5}, PM₁₀, O₃, NO₂, SO₂ and CO) are obtained from the Platform of Urban Ambient Air Quality Information of Shandong (<http://fb.sdem.org.cn:8801/AirDeploy.Web/AirQuality/MapMain.aspx>). As the necessary data for carrying out the assessment of population exposure

risk to PM_{2.5}, the grid data of PM_{2.5} with a resolution of 0.1° × 0.1° and the grid data of population with a resolution of 1 km × 1 km are cited to the Earthdata (2016) and the LandScan (2016), respectively.

Results and discussion

Interannual variations and distribution characteristics of air pollutant concentrations from 2014 to 2020 in Shandong

PM_{2.5}

The variation trends of concentrations of PM_{2.5} from 2014 to 2020 are shown in Fig. 2. As can be seen, the annual average concentrations of PM_{2.5} in 16 cities decrease from 40.8 to 104.8 μg/m³ in 2014 to 26.0–55.0 μg/m³ in 2020, with the annual decrease rate of 6.4–11.8%. However, the specific values of PM_{2.5} concentrations in inland cities are still higher than the concentration limit of Grade II (35 μg/m³) issued by China Ambient Air Quality Standards (CAAQS) (GB3095-2012).

The air pollution transmission channel cities are recognized as “2 + 26” cities firstly in February 2017 in the working scheme of air pollution control for Beijing-Tianjin-Hebei and surround regions in 2017, which is issued by MEEC. Subsequently, the regional work mechanism and measures of combined defense and control for air pollutions are built and implemented. Thus, the assessment period can be divided into two parts: 2014–2017 and 2017 to 2020. Specifically, the annual average PM_{2.5} concentrations of key cities, coastal cities and general cities in 2017 decrease by about 29.0%, 26.7% and 30.3%, compared with those in 2014, respectively. With the implementation of comprehensive prevention program of regional air pollution in key cities, the annual average PM_{2.5} concentrations of key cities decrease from 66.8 in 2017 to 51.5 μg/m³ in 2020, with decrease proportion of 22.2%, which is higher than those in coastal cities (16.8%) and other cities (13.9%).

As can be seen from Fig. 2, the annual average values of PM_{2.5} concentrations in 16 cities are all higher than their median values. Therein, the difference values between the mean and median of PM_{2.5} concentrations in 16 cities are estimated at about 8–18 μg/m³ and 6–13 μg/m³ in 2014 and 2020, respectively. Generally, the difference values present a downward trend in this period, which indicates that the extreme air pollution events resulting in significant PM_{2.5} concentrations are decreasing in numbers every year. Besides, the maximum values of PM_{2.5} concentrations in the most of the cities increase firstly (from 2014 to 2015) and then decrease (from 2015 to 2020). Taking Liaocheng as an example, the maximum value of

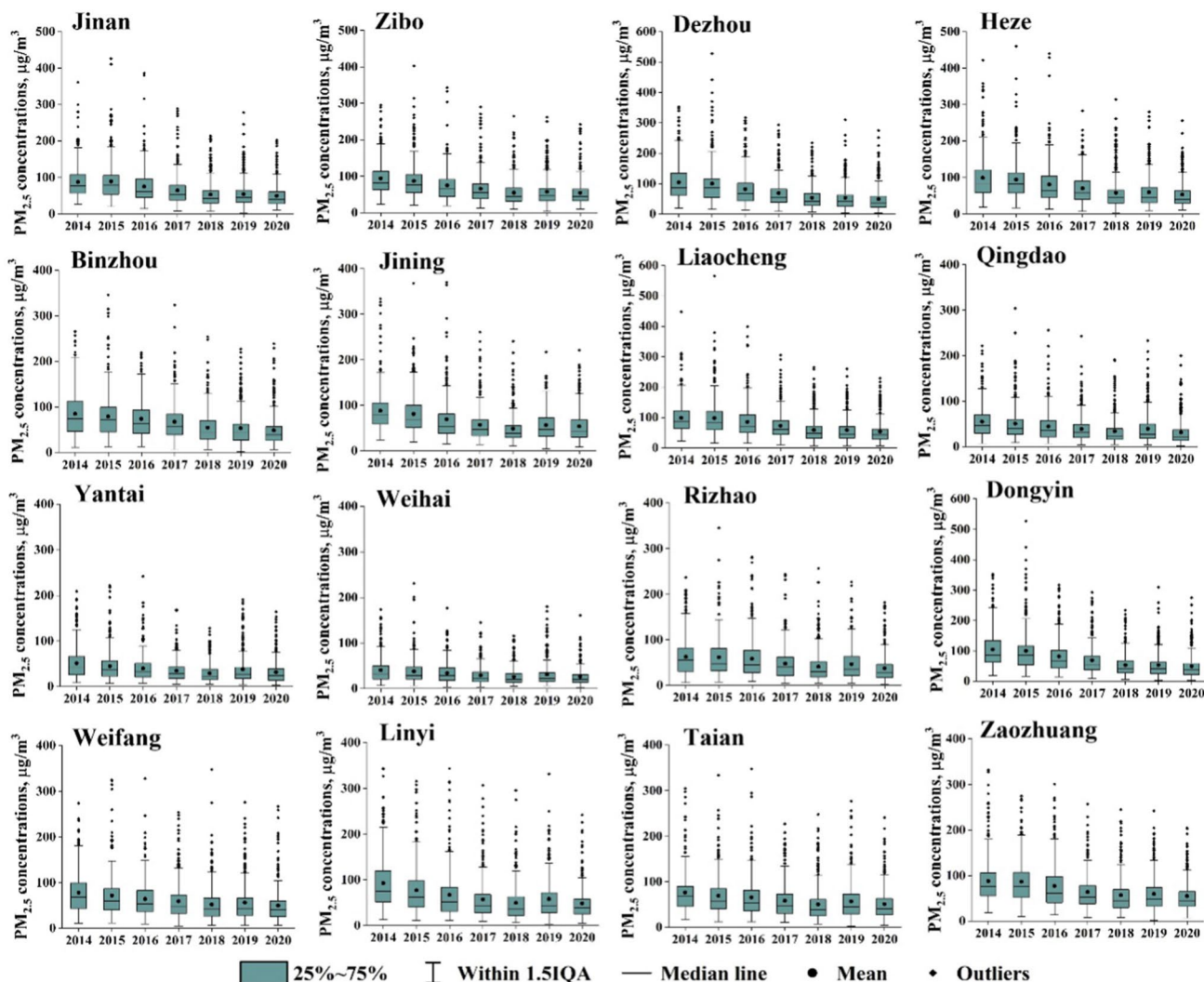


Fig. 2 The variation trends of concentrations of PM_{2.5} in 16 cities from Shandong province during 2014 to 2020

PM_{2.5} concentrations in 2015 is about 566 µg/m³, which is approximately 1.5 times higher than that in 2020.

Especially, the values of interquartile range (IQR) in different cities within 7 years have decreased steadily though there have been some fluctuations. The values of IQR in 2020 decrease by 18.2–53.0%, compared to those in 2014, for instance. These indicate that the pollution days with high PM_{2.5} concentration values reduce gradually because of the implementation of air pollution prevention and control actions, such as *Action Plan of Air Pollution Prevention and Control in Beijing–Tianjin–Hebei region and its surrounding areas* (Wang 2020). Furthermore, the decreasing IQR value demonstrates the air quality improvement in the future becomes more and more difficult based on conventional means. Therefore, carbon dioxide reduction brings about the energy composition adjustment and the industry structure optimization is the

available measures to mitigate conventional air pollutant emissions (Zhang and Lin 2012).

O₃

Ozone (O₃) is one of the secondary pollutants formed by chemical reactions of NO_x and VOCs under the action of sunlight and heat, which is complicated and difficult to control (Chen et al. 2020). Contrary to other five pollutants, the annual average MDA8 O₃ concentrations in Shandong exhibit an overall upward tendency during 2014 to 2020 (see Support Information (SI) Fig. S1). Specifically, the annual average MDA8 O₃ concentrations in key cities and general cities increase from 94.5 µg/m³ and 90.9 µg/m³ in 2014 to 109.9 µg/m³ and 111.6 µg/m³ in 2020, with an annual growth rate of 2.6% and 3.5%, respectively. Simultaneously, the annual average MDA8 O₃

concentrations in coastal cities fluctuate narrowly around $105 \mu\text{g}/\text{m}^3$. These are mainly due to the comprehensive results caused by many factors, including the significantly discharge of VOCs from anthropogenic sources, the lack of related studies on the formation mechanism of ozone, the depression of the heterogeneous absorption of HO_2 by aerosol with the decline of $\text{PM}_{2.5}$ concentrations and so on (Li et al. 2019a).

As we know, the standard deviation (SD) is usually used as the statistics parameter to characterize the dispersion degree of the data set. Due to lack of effective supervision and management for fugitive emission of VOCs from predominate sources (e.g., pharmaceutical industry, paint, ink and adhesive industry), the SD value of annual average MDA8 O_3 concentrations in 16 cities displays the decline trend during 2014 to 2020 in general. All of this shows that ozone pollution has become a common problem in all cities.

Mostly, the annual average values of MDA8 O_3 concentrations in 16 cities are higher than their median values in the corresponding years. For example, the annual average values of MDA8 O_3 concentrations and their median values are estimated at about $94\text{--}113 \mu\text{g}/\text{m}^3$ and $91\text{--}107 \mu\text{g}/\text{m}^3$ in 2020, respectively. Moreover, the values of IQR have showed the shrinking trends for 16 cities from 2014 to 2020 in general, which are consistent with the variation tendencies of IQR for $\text{PM}_{2.5}$. Compared with $\text{PM}_{2.5}$, there are fewer outliers ($> Q3 + 1.5 \text{ IQR}$) for MDA8 O_3 concentrations in the period of 2014 to 2020 (see SI Fig. S1). These indicate that there are few severely polluted events caused by the increase of ozone concentrations. However, ozone pollution has become an urgent problem affecting the air quality in summer. There are about 46–78 days for MDA8 O_3 concentrations from 7 cities (Binzhou, Dezhou, Heze, Jinan, Jining, Liaocheng and Zibo) exceeding the Grade II limit ($160 \mu\text{g}/\text{m}^3$) in 2020, for instance. Therefore, the collaborative prevention and control of ozone and fine particulate matter must be strengthened.

The interannual variations and distribution characteristics of concentrations of other four air pollutants (PM_{10} , NO_2 , SO_2 and CO) are described in SI Sects. 1 and 2. Meanwhile, the Pearson correlation is applied to determine the effects of NO_2 in the formation of O_3 with a significant level of < 0.05 (Rahman et al., 2019). Pearson's correlation coefficients between the annual concentrations MDA8 O_3 and NO_2 in different cities of Shandong are shown in Table S1. Ozone concentrations are negatively correlated with NO_2 in all cities. A similar conclusion is obtained by Song et al (2017) and Paraschiv et al (2020). Specifically, the Pearson correlation coefficients between MDA8 O_3 and NO_2 in key cities, coastal cities and general cities are estimated at about -0.35 , -0.21 and -0.28 , respectively. These are expected since the negatively correlated pollutant NO_x are ozone precursors, and therefore a rise in ozone concentrations is associated with a reduction in the levels of NO_x .

Analysis of monthly variation in air quality

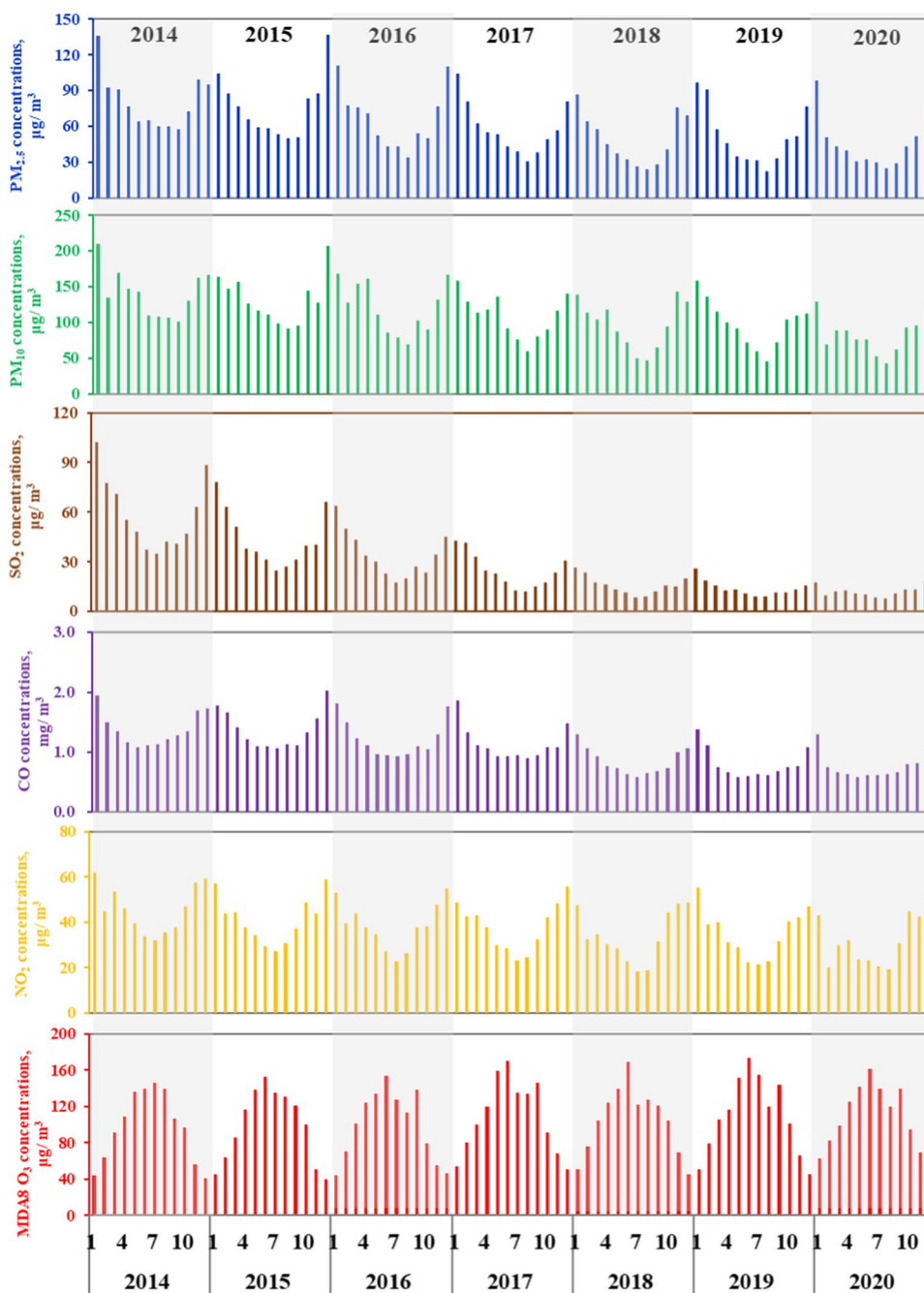
The monthly average concentrations of six air pollutants in Shandong from 2014 to 2020 are shown in Fig. 3. As can be seen, the monthly average concentrations of $\text{PM}_{2.5}$, PM_{10} , NO_2 , SO_2 and CO show the “u” type distributions from January to December in general, with the appearance of the maximum concentrations in winter months (January and December), and the minimum concentrations in summer months (June and August). These indicate that coal combustion is one of the main sources for above pollutants. On the contrary, the monthly average MDA8 O_3 concentrations exhibit the “n” type distribution at the same period. The maximum and minimum values of MDA8 O_3 concentrations are found in July and December, respectively (Song et al. 2017).

Besides winter months, high concentrations of PM_{10} are also found in March and April. This is mainly because large-scale strong sandstorms originated in Mongolia migrate to the southeastward with northwest airflow. Previous studies have indicated that both coal combustion source and motor vehicle are two main anthropogenic sources of NO_x (Zhou et al. 2021). Therefore, the concentrations of NO_x are correlated positively with coal consumptions and vehicle trips. Generally, the high concentrations of NO_2 are found in heating season. However, the concentration values of NO_2 in February are lower than these in other months during heating season of 2020. These are mainly due to the low traffic flow during the Spring Festival in the February. Especially, in order to prevent the spread of COVID-19, the central government of P.R. China issued the strictest prophylactic measures during January 26, 2020 to February 29, 2021. In this period, China's economic activity exhibits the sharp drop-off trend due to the implementation of home-based quarantine, stoppage and out-of-production. As a result, the monthly concentrations of $\text{PM}_{2.5}$, PM_{10} , SO_2 , CO and NO_2 decrease by about -44.7% , -49.5% , -48.4% , -32.1% and -48.2% in February 2020 year-on-year, respectively. Generally, the high monthly average MDA8 O_3 concentrations are concentrated in spring and summer. Therein, the highest value of monthly average MDA8 O_3 concentrations is found in June due to the intense solar radiation and high temperature. Especially, the MDA8 O_3 concentrations in September remain in high level in certain years, which are affected by higher temperature than those in the same period of the year (Yin et al. 2021).

The monthly AQICs of key cities, coastal cities and other cities from 2014 to 2020 are listed in SI Fig. S6. As a whole, the variation trends of monthly AQICs in different years are consistent. However, the monthly AQICs vary significantly in different month (see Fig. 4). As can be seen, the monthly AQICs of key cities, coastal cities and general cities in 2020 are estimated at about 3.6–8.2, 2.7–5.8 and 3.5–7.2,



Fig. 3 Monthly average concentrations of six air pollutants from 2014 to 2020



respectively. Although the comprehensive work of air pollution control and prevent has been done, the air quality of key cities is still worse than that of general cities due to the significant emissions of air pollutants from anthropogenic sources. In the context of carbon peak and carbon neutrality, artificial means of air pollution prevent in terms of the adjustment of industrial structure and energy composition in key cities should be implemented in the future.

Generally, the minimum monthly AQCI in 16 cities are found in August. January and December are the two months with the highest AQCI. Based on the analysis of

the proportions of I_i of air pollutants, the highest proportions of $I_{PM_{2.5}}$, $I_{PM_{10}}$ and I_{O_3} are found in January (36.6–40.9%), March (27.8–28.6%) and August (31.5–35.4%) in above three kinds of cities, respectively. These imply that $PM_{2.5}$, PM_{10} and O_3 are the key factors having adverse effect on air quality in winter, spring and summer, separately. In terms of autumn months, O_3 , PM_{10} and $PM_{2.5}$ are regarded as the primary pollutants in September, October and November, respectively. The main causes are listed as follows: suitable O_3 formation environment in September (e.g., high temperature), high fugitive dust discharges from high frequency and



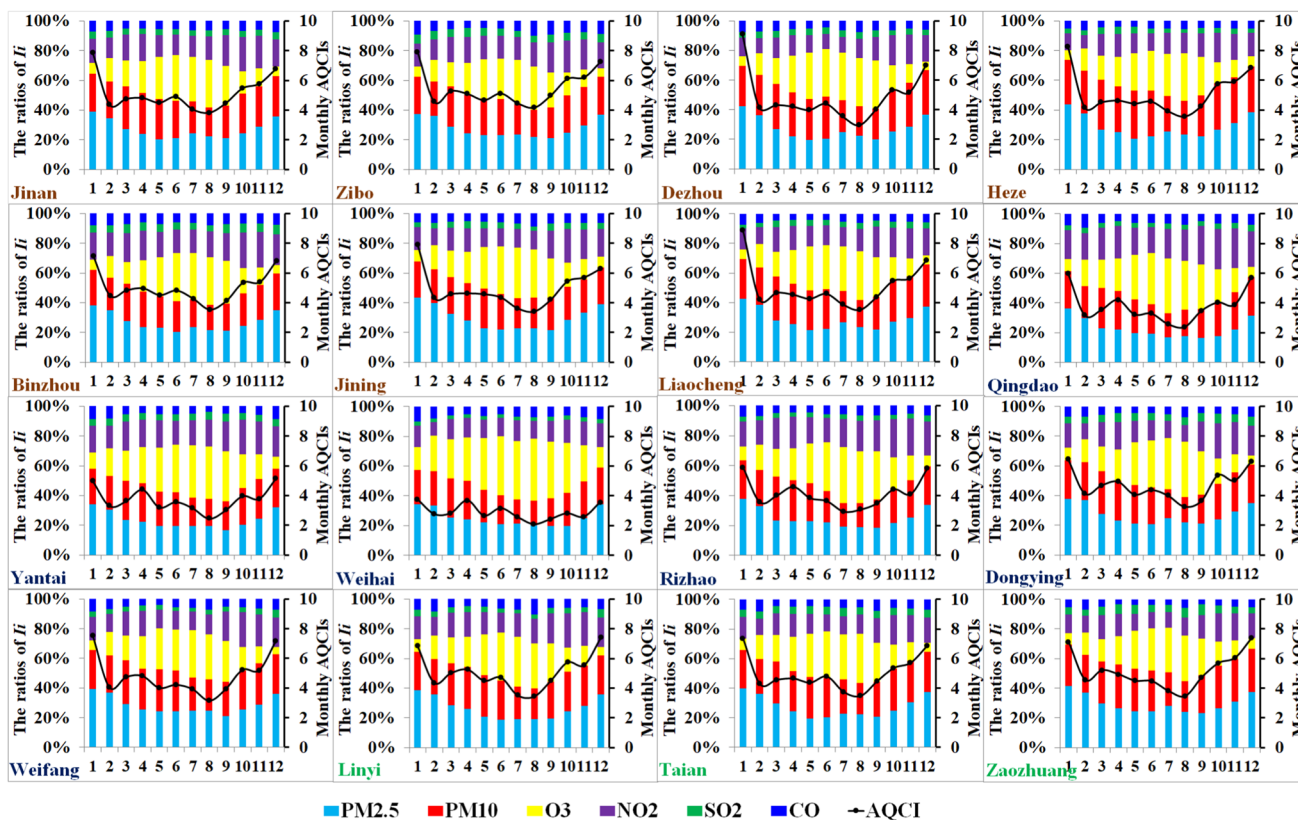


Fig. 4 The proportions of individual index (I_i) of air pollutants and their monthly AQCI in 16 cities in 2020

intensity usage of agricultural equipment in autumn harvest season and significant $PM_{2.5}$ emissions from tremendous coal combustion in central heating season.

In addition, the emission reduction of NO_x should be paid more attention in the future, the highest proportions of I_{NO_2} can be up to 20.8–22.9% in October in three kinds of cities, for instance.

Urban air quality and its primary pollutants in Shandong

The primary pollutant is defined to be the pollutant with the highest IAQI and the pollutant with the greatest contribution to air quality degradation. On the basis of *Technical Regulation on Ambient Air Quality Index*, air quality is defined to be six grades. The air quality grade is rated as good if IAQI is in the range (0, 50], moderate in the range [51, 100], lightly polluted in the range [101, 150], moderately polluted in the range [151, 200], heavily polluted in the range [201, 300] and severely polluted in the range (300, 500].

The air quality calendar in 16 cities during 2014 to 2020 is illustrated in SI Fig. S7. The average number of heavy polluted days and severe polluted days in 16 cities decreases significantly from 35 days in 2014 to 9 days in 2020. Meanwhile, the good and moderate rate of Shandong has increase

monotonously from 44.9% in 2014 to 69.1% in 2020 (MEES 2020).

The contribution rates of primary air pollutants in 16 cities in 2014 and 2020 are listed in Fig. 5. With the widely application of advanced air pollutant control devices (e.g., WFGD) and the greatly improvement in combustion efficiency based on the replacement and modification for coal fired boilers, there is no day for CO and SO_2 as the primary pollutant in 16 cities when AQI value is higher than 50 in 2020. However, the proportions of NO_2 as primary pollutant in Qingdao, Binzhou, Rizhao and Dongying are up to 5.2–9.0% in 2020, which implies that the emission reduction of NO_x from fossil fuel combustion and mobile source should be paid more attention in above coastal cities during the 14th Five Year Plan Period.

With the implementation of air pollution prevention and control action, the emissions of the regulated air pollutants (e.g., $PM_{2.5}$, PM_{10} , SO_2 , NO_x) from anthropogenic sources have been reduced substantially. As a result, the contribution rates of primary air pollutants in 16 cities have been changed greatly in 2020, compared to those in 2014. Although the total contribution rates of $PM_{2.5}$ and PM_{10} as the primary pollutants are still more than 50% in key cities and general cities during the days with AQI over 50, the day proportions of O_3 as the primary pollutant are the highest. Specifically,

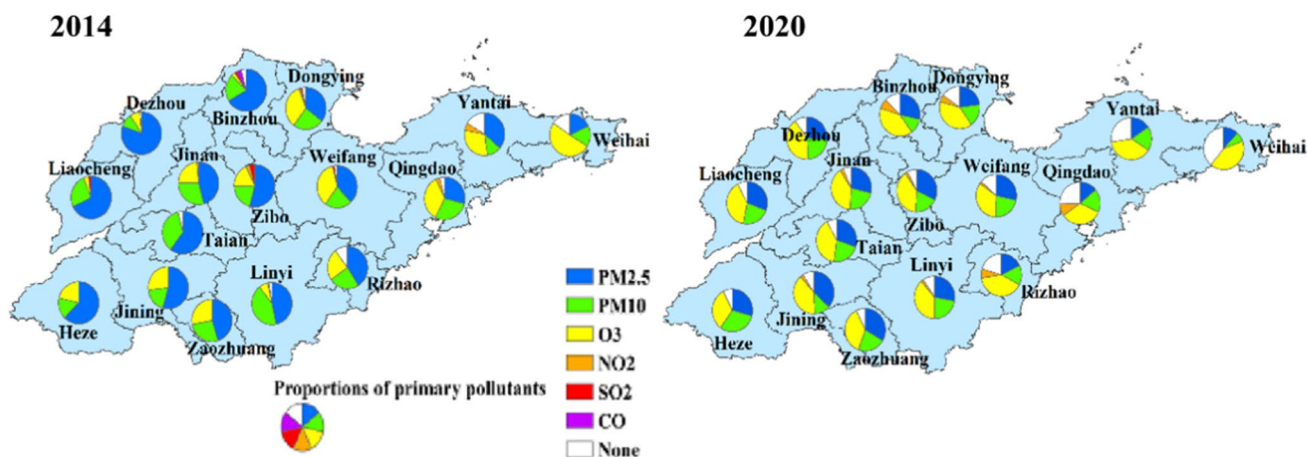


Fig. 5 The contribution rates of primary air pollutants in 16 cities in 2014 and 2020

the day proportions of O₃ as the primary pollutant are up to 38.7%, 37.9% and 38.4% in key cities, coastal cities and general cities, respectively. Besides, the proportions of days with AQI under 50 in key cities, coastal cities and general cities have increased from 1.1%, 8.6% and 2.1% in 2014 to 8.7%, 23.5% and 8.2% in 2020.

In order to clarify the actual pollution situation of individual pollutant, the days with IAQI over 100 for PM_{2.5}, PM₁₀ and O₃ of 16 cities in 2014 and 2020 are counted elaborately. Please see SI Sect. 3 for more details.

Population exposure risk to PM_{2.5} in Shandong

The spatial distribution of population exposure risk to PM_{2.5} in Shandong in 2016 and 2020 is shown in Fig. 6. In this study, the PM_{2.5} population exposure risk levels are divided into six categories, including extremely safe ($R_i=0$), safe ($0 < R_i \leq 1$), relatively safe ($1 < R_i \leq 2$), relatively dangerous ($2 < R_i \leq 3$), dangerous ($3 < R_i \leq 5$) and extremely dangerous ($R_i > 5$) (Zhang and Pan 2020b).

Based on the statistics analysis of grid data of R_i , we find that the average values of R_i in key cities, coastal cities and

general cities decrease from 2.4, 1.4 and 2.1 in 2016 to 1.6, 1.0 and 1.6 in 2020, with an annual decreasing rate of 9.0%, 6.6% and 6.9%, respectively. Nevertheless, there are substantial amount grids listed in the region with high population exposure risk ($R_i > 2$). Specifically, the proportions of grid amount with high population exposure risk ($R_i > 2$) in key cities, coastal cities and general cities decrease from 40.0%, 15.6% and 34.4% in 2016 to 20.6%, 10.3% and 22.6% in 2020, respectively. Among them, the amount of extremely dangerous grids ($R_i > 5$) in key cities, coastal cities and general cities account for approximately 3.5%, 2.6% and 4.2% of the sum of grids in study area in 2020. In terms of the population exposed to high risk areas ($R_i > 2$), the specific proportion values are estimated at about 55.2%, 49.9% and 51.1% in key cities, coastal cities and general cities in 2020, respectively. Especially, the proportions of population exposed to extremely dangerous areas in three kinds of cities are up to 25%. These imply that high pollution areas are also the regions with high population density.

With respect to the spatial distribution characteristics of R_i , the extremely dangerous areas are concentrated in main urban areas, industrial areas and central district of counties

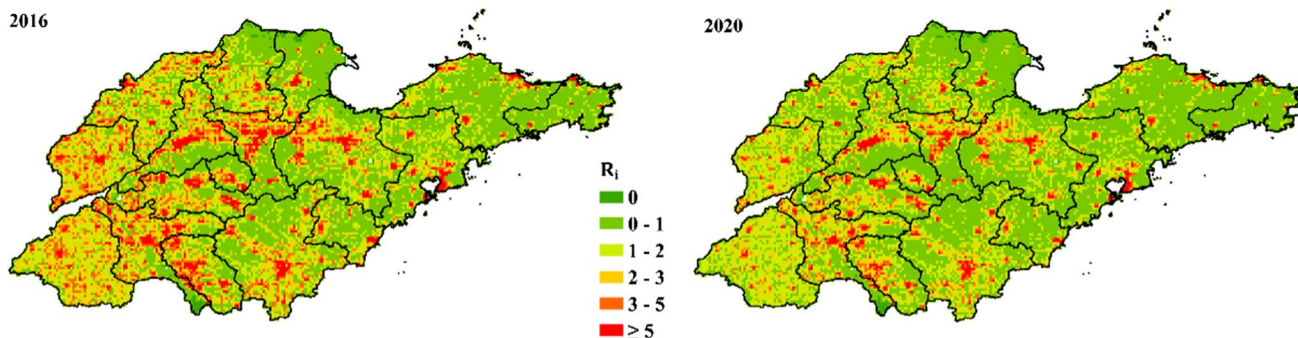


Fig. 6 Spatial distribution of population exposure risk to PM_{2.5} in 2016 and 2020

in general. These are mainly because of high population density and serious pollution of PM_{2.5} in above areas.

As we know, the air pollution causes the adverse effects on human health and the health-related economic factors, such as human health costs and labor productivity, while the decrease of PM_{2.5} concentrations can provide sustainable health and economic benefits to the cities (Martinez et al. 2018).

Conclusions

Owing to the implementation of air pollution prevention and control actions for haze, the annual average concentrations of PM_{2.5}, PM₁₀, SO₂, NO₂ and CO decrease from 80.9 µg/m³, 140.9 µg/m³, 59.0 µg/m³, 45.7 µg/m³ and 1.4 mg/m³ in 2014 to 46.3 µg/m³, 82.9 µg/m³, 12.0 µg/m³, 31.5 µg/m³ and 0.8 mg/m³ in 2020, with an annual decrease rate of 8.9%, 8.5%, 23.3%, 6.0% and 9.4%, respectively. However, the annual average MDA8 O₃ concentrations increase from 97.9 in 2014 to 107.4 µg/m³ in 2020, with an annual growth rate of 1.6%. By 2020, the day proportions of O₃ as the primary pollutant are the highest in three kinds of cities. Generally, the monthly average concentrations of MDA8 O₃ and other five air pollutants (PM_{2.5}, PM₁₀, NO₂, SO₂ and CO) show the “n” and “u” type distributions from January to December in 2020, separately. Due to the impact of COVID-19, the monthly average concentrations of PM_{2.5}, PM₁₀, NO₂, SO₂ and CO in February 2020 decrease by 32.1–49.5% year-on-year.

According to the box diagrams of daily concentrations of six air pollutants, the IQR values of pollutant concentrations show the shrinking trends for 16 cities from 2014 to 2020 in general, which imply that the air quality improvement in the future becomes more and more difficult based on conventional means. However, the energy composition adjustment and the industry structure optimization are the available measures to mitigate air pollutant emissions in the context of low-carbon economy.

There are still about 50% of population exposed to high risk regions ($R_i > 2$), which are principally concentrated in main urban areas and industrial areas. These indicate that the exposure risk of air pollutants should be taken into account during the optimization of industrial structure distribution and functional area construction in the city.

Supplementary Information The online version contains supplementary material available at <https://doi.org/10.1007/s13762-022-04651-5>.

Acknowledgements This work is jointly funded by the National Natural Science Foundation of China (21707075 and 41905111), Shandong Provincial Natural Science Foundation (ZR2019BD030), the National Training Program on Undergraduate Innovation and Entrepreneurship (201910431041) and Qilu University of Technology Teaching Reform Project (2019yb36).

Declarations

Conflict of interest The author declares that no conflict of interest.

References

- Chen ZY, Li RY, Chen DL et al (2020) Understanding the causal influence of major meteorological factors on ground ozone concentrations across China. *J Cleaner Prod* 242:118498. <https://doi.org/10.1016/j.jclepro.2019.118498>
- Earthdata (2016) Global Annual PM_{2.5} Grids from MODIS, MISR and SeaWiFS Aerosol Optical Depth (AOD) with GWR. Retrieved from <https://cmr.earthdata.nasa.gov/search/concepts/C1513365323-SEDAC.html>. Accessed 26 June 2020
- Gao C, Xiu AJ, Zhang XL et al (2020) Spatiotemporal characteristics of ozone pollution and policy implications in Northeast China. *Atmos Pollut Res* 11(2):357–369. <https://doi.org/10.1016/j.apr.2019.11.008>
- Huang Y, Yan Q, Zhang C (2018) Spatial-temporal distribution characteristics of PM_{2.5} in China in 2016. *J Geovisualization Spatial Anal* 2(2):12. <https://doi.org/10.1007/s41651-018-0019-5>
- LandScan (2016) LandScan Global. Retrieved from <https://landscan.ornl.gov/landscan-datasets>. Accessed 7 June 2020
- Li K, Jacob DJ, Liao H et al (2019a) A two-pollutant strategy for improving ozone and particulate air quality in China. *Nat Geosci* 12(11):906–910. <https://doi.org/10.1038/s41561-019-0464-x>
- Li R, Wang ZZ, Cui LL et al (2019b) Air pollution characteristics in China during 2015–2016: spatiotemporal variations and key meteorological factors. *Sci Total Environ* 648:902–915. <https://doi.org/10.1016/j.scitotenv.2018.08.181>
- Liao TT, Gui K, Jiang WT et al (2018) Air stagnation and its impact on air quality during winter in Sichuan and Chongqing, southwestern China. *Sci Total Environ* 635:576–585. <https://doi.org/10.1016/j.scitotenv.2018.04.122>
- Liu J, Han YQ, Tang X et al (2016) Estimating adult mortality attributable to PM_{2.5} exposure in China with assimilated PM_{2.5} concentrations based on a ground monitoring network. *Sci Total Environ* 568:1253–1262. <https://doi.org/10.1016/j.scitotenv.2016.05.165>
- Liu XP, Zou B, Feng HH et al (2020) Anthropogenic factors of PM_{2.5} distributions in China’s major urban agglomerations: a spatial-temporal analysis. *J Cleaner Prod* 264:121709. <https://doi.org/10.1016/j.jclepro.2020.121709>
- Liu M, Saari RK, Zhou GX et al (2021) Recent trends in premature mortality and health disparities attributable to ambient PM_{2.5} exposure in China: 2005–2017. *Environ Pollut* 279:116882. <https://doi.org/10.1016/j.envpol.2021.116882>
- Ma T, Duan FK, He KB et al (2019) Air pollution characteristics and their relationship with emissions and meteorology in the Yangtze River Delta region during 2014–2016. *J Environ Sci* 83:8–20. <https://doi.org/10.1016/j.jes.2019.02.031>
- Martinez GS, Spadaro JV, Chapizanis D et al (2018) Health impacts and economic costs of air pollution in the metropolitan area of Skopje. *Int J Environ Res Public Health* 15(4):1–11. <https://doi.org/10.3390/ijerph15040626>
- Ministry of Ecology and Environment of Beijing (MEEB) (2020) Beijing Ecology and Environment Statement 2020. Retrieved from <http://sthjj.beijing.gov.cn/bjhrb/resource/cms/article/1718882/10985106/2021051214515686015.pdf>. Accessed 16 July 2020
- Ministry of Ecology and Environment of China (MEEC) (2016) China Environmental State Bulletin 2016. Retrieved from <https://www.mee.gov.cn/hjzl/sthjzk/zghjzkgb/201706/P020170605833655914077.pdf>. Accessed 18 May 2020
- Ministry of Ecology and Environment of China (MEEC) (2020) China Environmental State Bulletin 2020. Retrieved from <https://www.mee.gov.cn/hjzl/sthjzk/zghjzkgb/202106/P020210605833655914077.pdf>. Accessed 18 May 2020



- mee.gov.cn/hjzl/sthjzk/zghjzkgb/202105/P020210526572756184785.pdf. Accessed 19 May 2020
- Ministry of Ecology and Environment of Shandong (MEES) (2020) Shandong Environmental State Bulletin 2020. Retrieved from <http://xxgk.sdein.gov.cn/wryhjgxxgk/zlkz/zkgb/202106/P020210603483891736412.pdf>. Accessed 19 May 2020
- National Statistics Bureau of China (NSBC) (2021) China Statistical Yearbook 2021. Retrieved from <http://www.stats.gov.cn/tjsj/ndsj/2021/indexch.htm>. Accessed 6 Sep 2021
- Paraschiv S, Barbuta-Misu N, Paraschiv SL (2020) Influence of NO₂, NO and meteorological conditions on the tropospheric O₃ concentration at an industrial station. *Energy Rep* 6:231–236. <https://doi.org/10.1016/j.egy.2020.11.263>
- Rahman A, Luo C, Khan MHR et al (2019) Influence of atmospheric PM_{2.5}, PM₁₀, O₃, CO, NO₂, SO₂, and meteorological factors on the concentration of airborne pollen in Guangzhou. *China Atmos Environ* 212:290–304. <https://doi.org/10.1016/j.atmosenv.2019.05.049>
- Song CB, Wu L, Xie YC et al (2017) Air pollution in China: Status and spatiotemporal variations. *Environ Pollut* 227:334–347. <https://doi.org/10.1016/j.envpol.2017.04.075>
- Shandong Provincial Bureau of Statistics (SPBS) (2021) Shandong Statistical Yearbook 2020. Retrieved from <http://tjj.shandong.gov.cn/>. Accessed 6 Sep 2021
- Stafoggia M, Cesaroni G, Peters A et al (2014) Long-term exposure to ambient air pollution and incidence of cerebrovascular events: results from 11 European cohorts within the ESCAPE Project. *Environ Health Perspect* 122(9):919–925. <https://doi.org/10.1289/ehp.1307301>
- Wang P (2020) China's air pollution policies: progress and challenges. *Curr Opin Environ Sci Health* 19:100227. <https://doi.org/10.1016/j.coesh.2020.100227>
- Wang QQ, Li J, Yang JX et al (2020) Seasonal characterization of aerosol composition and sources in a polluted city in Central China. *Chemosphere* 258:127310. <https://doi.org/10.1016/j.chemosphere.2020.127310>
- Xiao CC, Chang M, Guo PK et al (2020) Characteristics analysis of industrial atmospheric emission sources in Beijing-Tianjin-Hebei and Surrounding Areas using data mining and statistics on different time scales. *Atmos Pollut Res* 11(1):11–26. <https://doi.org/10.1016/j.apr.2019.08.008>
- Ye WF, Ma ZY, Ha XZ et al (2018) Spatiotemporal patterns and spatial clustering characteristics of air quality in China: a city level analysis. *Ecol Indic* 91:523–530. <https://doi.org/10.1016/j.ecolind.2018.04.007>
- Yin H, Liu C, Hu Q et al (2021) Opposite impact of emission reduction during the COVID-19 lockdown period on the surface concentrations of PM_{2.5} and O₃ in Wuhan, China. *Environ Pollut* 289:117899. <https://doi.org/10.1016/j.envpol.2021.117899>
- Zhang CG, Lin Y (2012) Panel estimation for urbanization, energy consumption and CO₂ emissions: a regional analysis in China. *Energy Policy* 49:488–498. <https://doi.org/10.1016/j.enpol.2012.06.048>
- Zhang LL, Pan JH (2020a) Estimation of PM_{2.5} mass concentrations in Beijing–Tianjin–Hebei region based on geographically weighted regression and spatial downscaling method. *J Indian Soc Remote Sens* 48(12):1691–1703. <https://doi.org/10.1007/s12524-020-01193-6>
- Zhang LL, Pan JH (2020b) Spatial-temporal pattern of population exposure risk to PM_{2.5} in China. *Chin Environ Sci* 40(1):1–12. <https://doi.org/10.19674/j.cnki.issn1000-6923.2020b.0001>
- Zhang A, Lin JH, Chen WH et al (2021) Spatial-temporal distribution variation of ground-level ozone in China's Pearl River Delta metropolitan region. *Int J Environ Res Public Health* 18(3):1–13. <https://doi.org/10.3390/ijerph18030872>
- Zhou Y, Cheng SY, Chen DS et al (2015) Temporal and spatial characteristics of ambient air quality in Beijing. *China Aerosol Air Qual Res* 15(5):1868–1880. <https://doi.org/10.4209/aaqr.2014.11.0306>
- Zhou M, Jiang W, Gao W et al (2021) Anthropogenic emission inventory of multiple air pollutants and their spatiotemporal variations in 2017 for the Shandong Province. *China Environ Pollut* 288:117666. <https://doi.org/10.1016/j.envpol.2021.117666>

Springer Nature or its licensor (e.g. a society or other partner) holds exclusive rights to this article under a publishing agreement with the author(s) or other rightsholder(s); author self-archiving of the accepted manuscript version of this article is solely governed by the terms of such publishing agreement and applicable law.

